Challenge of human Jurkat T-cells with the adenylate cyclase activator forskolin elicits major changes in cAMP phosphodiesterase (PDE) expression by up-regulating PDE3 and inducing PDE4D1 and PDE4D2 splice variants as well as down-regulating a novel PDE4A splice variant

Suat ERDOGAN* and Miles D. HOUSLAY†

Molecular Pharmacology Group, Division of Biochemistry and Molecular Biology, Institute of Biomedical and Life Sciences, Wolfson Building, University of Glasgow, Glasgow G12 8QQ, Scotland, U.K.

The cAMP phosphodiesterase (PDE) 3 and PDE4 isoforms provide the major cAMP-hydrolysing PDE activities in Jurkat T-cells, with additional contributions from the PDE1 and PDE2 isoforms. Challenge of cells with the adenylate cyclase activator forskolin led to a rapid, albeit transient, increase in PDE3 activity occurring over the first 45 min, followed by a sustained increase in PDE3 activity which began after ~ 3 h and continued for at least 24 h. Only this second phase of increase in PDE3 activity was blocked by the transcriptional inhibitor actinomycin D. After ~ 3 h of exposure to forskolin, PDE4 activity had increased, via a process that could be inhibited by actinomycin D, and it remained elevated for at least a 24 h period. Such actions of forskolin were mimicked by cholera toxin and 8-bromo-cAMP. Forskolin increased intracellular cAMP concentrations in a time-dependent fashion and its action was enhanced when PDE induction was blocked with actinomycin D. Reverse transcription (RT)-PCR analysis, using generic primers designed to detect transcripts representing enzymically active products of the four PDE4 genes, identified transcripts for PDE4A and PDE4D but not for PDE4B or PDE4C in untreated Jurkat T-cells. Forskolin treatment did not induce transcripts for either PDE4B or PDE4C; however, it reduced the RT-PCR signal for PDE4A transcripts and markedly enhanced that for PDE4D transcripts. Using RT-PCR primers for PDE4 splice variants, a weak signal for PDE4D1 was evident in control cells whereas, in forskolin-treated cells, clear signals for both PDE4D1 and PDE4D2 were detected. RT-PCR analysis of the PDE4A species indicated that it was not the PDE4A isoform PDE-46 (PDE4A4B). Immunoblotting of control cells for PDE4 forms identified a single PDE4A species of ~ 118 kDa, which migrated distinctly from the PDE4A4B isoform PDE-46, with immunoprecipitation analyses showing that it provided all of the PDE4 activity in control cells. Forskolin treatment led to a marked decrease of this novel PDE4A species and allowed the detection of a strong signal for an ~ 67 kDa PDE4D species, suggested to be PDE4D1, but did not induce PDE4B and PDE4C isoforms. Elevation of intracellular cAMP concentrations in Jurkat T-cells thus exerts a highly selective effect on the transcriptional activity of the genes encoding the various PDE4 isoforms. This leads to the down-regulation of a novel PDE4A splice variant and the induction of PDE4D1 and PDE4D2 splice variants, leading to a net increase in the total PDE4 activity of Jurkat T-cells.

INTRODUCTION

cAMP is a key second messenger which serves to regulate a variety of key processes in cells. It is synthesized through the action of adenylate cyclase and its sole route of degradation is through the action of a family of cAMP phosphodiesterases (PDEs). This activity is provided by a multigene family composed of the PDE1 (Ca^{2+}/calmodulin-stimulated) enzymes, the PDE2 (cGMP-stimulated) enzymes, the PDE3 (cGMP-inhibited) enzymes and the PDE4 and PDE7 cAMP-specific enzymes [1–5]. Such a complex gene family provides a variety of enzymes with highly distinctive regulatory properties, conferring controls on cAMP metabolism which appear to be tailored for specific cell types.

Recently there has been considerable interest in the development of inhibitors of PDE4 isoenzymes for the treatment of inflammatory diseases, in particular asthma [6–8]. The rationale for this is that chronically elevated cAMP levels will attenuate the functioning of cells involved in mediating inflammatory responses. In the past, however, considerable evidence has accrued showing that when various cells have chronically increased cAMP levels this induces an increase in PDE activity (e.g. see [3]). However, only recently has the true extent of the diversity of PDE forms become apparent. This is especially true for the PDE4 enzyme family, which is composed of products emanating from four distinct genes (PDE4A, PDE4B, PDE4C and PDE4D), with additional complexity arising from multiple splicing [2,3,9]. Indeed, Conti and co-workers were the first to demonstrate that specific PDE forms could be induced by cAMP elevation, namely elevation of transcripts for PDE4D splice variants in Sertoli cells [10,11]. More recently, however, up-regulation of PDE4 isoforms upon chronic elevation of cAMP levels has been noted in monocytic cells, which have a key involvement in inflammatory responses [12,13].

T-cells play key roles in regulating immune responses. It is generally accepted that cAMP exerts negative modulatory effects

Abbreviations used: PDE, cAMP phosphodiesterase; IBMX, isobutylmethylxanthine; EHNA, erythro-9-(2-hydroxy-3-nonyl)adenine (previously known as MEP-1); GST, glutathione S-transferase; RT-PCR, reverse transcription-PCR.

* Permanent address: Department of Biochemistry, Faculty of Veterinary Medicine, University of Mustafa Kemal, Antakya, Turkey.

† To whom correspondence and reprint requests should be directed.

on T-cell proliferation [14,15], can stimulate thymic apoptosis [16] and can inhibit interleukin-2 production [17,18], although the precise molecular mechanisms that underlie such effects are not understood in detail. However, consistent with such a notion, leukaemic lymphocytes appear to have lowered cAMP levels, and this may be attributable to the elevated PDE activity that has been observed in such instances (e.g. see [4]). One possible route through which cAMP might exert an inhibitory effect on cell growth is that, in many cells, protein kinase A can seemingly inhibit the activation of mitogen-activated protein (MAP) kinase by eliciting the phosphorylation and inactivation of C-Raf [19–21]. However, there is evidence to suggest that this does not occur in T-cells, but that elevated cAMP levels serve to inhibit c-Jun N-terminal kinase [22]. As T-cell activation, including interleukin-2 gene activation, requires the integration of the Raf-1 and c-Jun N-terminal kinase pathways, then a block in either will lead to an inhibitory effect (e.g. see [22]). Little is known, however, about the effects of a chronic elevation of intracellular cAMP concentrations on the expression of specific PDE isoforms in T-cells and, in particular, on the control of expression of PDE4 splice variants. Here we examine the effect on cellular PDE activity of culturing a human Jurkat T-cell line with the adenylate cyclase activator forskolin. We show that such treatment leads to a profound and sustained increase in PDE activity with marked, selective, changes occurring in the expression of splice variants of the genes encoding PDE4A and PDE4D.

MATERIALS AND METHODS

Materials

Forskolin and Pansorbin were from Calbiochem (Cambridge, U.K.). RPMI-1640 medium, fetal calf serum, L-glutamine, streptomycin, penicillin and EDTA were from Gibco/BRL (Paisley, U.K.). Actinomycin D, benzamidine hydrochloride, PMSF, aprotinin, pepstatin A, antipain, EGTA, cAMP, cGMP, Dowex 1X8-400 (chloride form; 200–400 mesh), 3-isobutyl-1-methylxanthine (IBMX), snake venom (*Ophiophagus hannah*), bovine brain calmodulin, Tween-80, BSA, 8-bromo cAMP, cholera toxin, digitonin, Tri-reagent and ethidium bromide were from Sigma Chemical Co. (Poole, Dorset, U.K.). [^{3}H]cAMP and anti-mouse IgG conjugated to horseradish peroxidase were from Amersham International (Amersham, Bucks., U.K.). Leupeptin was from Peptide Research Foundation (Scientific Marketing Associates, London, U.K.). Dithiothreitol was from Boehringer (Lewes, E. Sussex, U.K.). Triethanolamine was from BDH (Glasgow, U.K.). Bradford reagent and acrylamide were from Bio-Rad. DMSO was from Koch-Light Ltd. (Haverhill, U.K.). Horseradish peroxidase-conjugated anti-rabbit IgG was from SAPU. Rolipram {4-[3-(cyclopentoxyl)-4-methoxyphenyl]-2-pyrrolidone} was generously donated by Schering Aktiengesellschaft (Berlin 65, Germany). EHNA [erythro-9-(2-hydroxy-3-nonyl)adenine] was a gift from Dr. T. Podzuweit (Max Planck Institute, Bad Nauheim, Germany). Cilostimide {4,5-dihydro-6-[4-(1H-imidazol-1-yl)phenyl]-5-methyl-3(2H)-pyrazone} was from Pfizer Central Research (Sandwich, Kent, U.K.). cDNAs encoding human PDE4D1 and human PDE4A4B (PDE-46) were kindly donated by Dr. G. Bolger (University of Utah, Salt Lake City, UT, U.S.A.) [23], and that encoding human PDE4C [24] was a gift from Dr. Peter Engels (Sandoz, Basel, Switzerland). The cDNA encoding PDE4A4C (h6.1) has been reported previously by us [25,26]. *Taq* polymerase, *Taq* buffer and deoxyribonucleoside triphosphates were from Promega (Southampton, U.K.). A first-strand cDNA synthesis kit was from Pharmacia Biotech.

Cell culture and stimulation of Jurkat cells

The human T-cell leukaemia line Jurkat (J6) was cultured in RPMI-1640 medium supplemented with 5% heat-inactivated fetal bovine serum, 100 units/ml penicillin, 100 μg/ml streptomycin and 2 mM L-glutamine at 37 °C in 5% CO_2 in air. Twice weekly, the cells were split, diluting cells into fresh prewarmed medium in 75 cm^2 tissue culture flasks (1:5 dilution) under sterile conditions. Jurkat T-cells (2×10^6 cells/ml) were harvested by centrifugation (5 min, 1000 ***g***, at room temperature) and resuspended in culture medium. They were then incubated as indicated for the particular experimental procedure. Where forskolin was added, this was dissolved in 100% DMSO at a concentration of 0.1 M and then added to cells to yield a final concentration of 0.1 mM forskolin [final DMSO concentration of 0.1%; alone, this had no effect on cell PDE activity/expression (results not shown)]. Cells were incubated with forskolin, as a routine, for 9 h unless indicated otherwise. When actinomycin D was added, this was dissolved in RPMI-1640 medium and added together with forskolin at the start of the incubation period. Where indicated, cells were treated similarly with either 8-bromo-cAMP (100 μM final concentration) dissolved in water or cholera toxin (1 μg/ml).

Disruption of Jurkat cells

Following incubation, cells were harvested by centrifugation as described above, then washed twice with serum-free RPMI-1640 medium under the same conditions before being resuspended using a glass mortar and Teflon pestle in ice-cold homogenization buffer. This buffer comprised 10 mM Tris/HCl, final pH 7.4, containing 0.25 M sucrose, 1 mM EDTA and 0.1 mM dithiothreitol, and was supplemented with a protease inhibitor cocktail of 2 mM concentrations of each of antipain, pepstatin A, aprotinin, leupeptin and benzamidine, together with 0.1 mM PMSF and the detergent digitonin (0.5 mg/ml). This extract was left on ice for 8 min prior to use. Such a procedure released all ($> 98\%$) of lactate dehydrogenase activity associated with these cells and also rendered soluble all ($> 98\%$) PDE activity. Samples then either were taken for immediate assay of PDE activity or were snap-frozen in liquid nitrogen and stored at -80 °C until use; such storage had no effect on the results.

Transfection of COS-7 cells

COS-7 cells were cultured and transfected as described elsewhere in some detail [27].

Protein determination

Protein was routinely measured by the method of Bradford [28], with BSA as a standard.

PDE assay

PDE activity was determined by a modification [29,30] of the two-step radioactive assay [31] using [^{3}H]cAMP and unlabelled cAMP to give final concentration of 1 μM cAMP as substrate in 20 mM Tris/HCl and 10 mM $MgCl_2$ (final pH 7.4) (PDE buffer). Appropriate samples of enzyme extracts, to give linear time courses, were incubated in this assay mixture for 10 min at 30 °C and the reaction was terminated by boiling for 2 min. Rolipram, IBMX and cilostimide were dissolved in DMSO at concentrations

such that the final DMSO concentration was 0.1 %, which was demonstrated to have no effect on PDE activities. EHNA was dissolved in water. Activities are expressed as the specific activity (pmol/min per mg of protein; mean ± S.D.) unless indicated otherwise. Dose–effect studies were analysed by curve fitting to the appropriate equation using the Levenberg–Marquardt algorithm with the KaleidaGraph package for the Apple Macintosh in order to derive IC_{50} values and Hill coefficients together with associated errors.

Measurement of intracellular cAMP concentrations

Cell incubations with ligands were stopped by adding 100 μl of 2 % $HClO_4$. The precipitated protein was pelleted by centrifuging the samples in a Beckman Microfuge (13000 ***g***) for 2 min. The supernatant was neutralized with KOH/triethanolamine (2 M/0.5 M) before centrifuging again to remove the $KClO_4$ precipitate. The cAMP content of the supernatant was determined using a cAMP binding protein prepared from bovine adrenal glands as described previously by us [32].

SDS/PAGE analysis

Samples were dissolved in Laemmli [33] buffer and immediately boiled for 3 min as described by Laemmli [33] prior to electrophoresis on an 8 % acrylamide gel [running buffer 25 mM Tris, 0.19 M glycine, 0.1 % (w/v) SDS] at 7 mA/gel overnight or 60 mA/gel for 3–4 h with cooling.

Immunoblotting

Proteins were transferred from the gel to nitrocellulose paper using a constant current at 90 V for 90 min in a Bio-Rad Transblot apparatus. The buffer used was 25 mM Tris and 0.19 M glycine/methanol (4:1, v/v). After blotting, the nitrocellulose paper was washed twice with TBS/Tween 80 (500 mM NaCl, 20 mM Tris, final pH 7.4, with 0.2 % Tween 80) for 10 min and washed repeatedly with TBS. Non-specific binding to filters was blocked by incubation in 5 % non-fat dried milk powder/TBS at room temperature for 90 min. Using polyclonal antisera specific for PDE4A, blots were then washed as above and incubated for 90 min at room temperature with a 1:300 dilution (in TBS containing 1 % non-fat dried milk powder) of polyclonal anti-PDE4A rabbit serum. After further washes with TBS, blots were incubated for 90 min with 1 % non-fat dried milk powder containing 1:1000-diluted anti-rabbit peroxidase-linked IgG with an enhanced chemiluminescence (ECL) Western blotting visualization protocol (Amersham). The anti-PDE4A sera used were the anti-peptide antiserum described previously by us [27,34] and one developed against a C-terminal human PDE4A fusion protein which is reported elsewhere [35]. Briefly, a 300 bp DNA fragment encoding amino acids 541–639 of h6.1 (GenBank accession no. U18087; [25]), which is identical to amino acids 788–886 of the human PDE4A species PDE-46 (GenBank accession no. L20965; [23]), was generated by using the PCR primers Sense-6.1 (CGTGGGATCCGCAGTGCACC) and Antisense-6.1 (GTCACGATGAATTCTCAGGTAGGGTCTCC). This was then cloned into the inducible bacterial expression vector pGEX-3X to create an in-frame fusion with the glutathione S-transferase (GST) gene in a plasmid which we have called pGEX-3X-(788–886)-PDE46. The induced and purified fusion protein [GST-(788–886)-PDE46] was used to immunize New Zealand White rabbits to yield antisera referred to as PAb24/GST-(788–886)-PDE46 and PAb23/GST-(788–886)-PDE46. Rabbits were also immunized with native GST, with the resultant antiserum referred to as GST.

Immunoblotting was also carried out using monoclonal antibodies designed to be specific for particular PDE4 families (kindly donated by Dr. K. Ferguson, ICOS Corp., Seattle, WA, U.S.A.). They were raised against GST fusion proteins formed from portions of the C-terminal ends found to be unique to each of the PDE4 families and which appear to be common to all active proteins produced by a particular PDE4 family isoform as diversity arises among active forms by 5′ domain swopping only [2]. The monoclonal antibodies used were (i) the PDE4A-specific species 66C12H, which can recognize the peptide EEFVVAVSHSS found uniquely near the C-terminus of PDE-46 (residues 800–810) [23], and (ii) 61D10E, which is PDE4D-specific and can recognize the peptide TQDSESTEIPLDEQVEE found near the C-terminus of all known active PDE4D splice variants (e.g. residues 634–650 in PDE-43; residues 770–786 in PDE-39) but not in any other PDE4 classes [23]. Detection using monoclonal antibodies was achieved by using a 1:2000 dilution for 90 min, after which visualization was achieved by enhanced chemiluminescence using a 1:1000 dilution of a sheep anti-mouse Ig linked to horseradish peroxidase. Screening against extracts from COS cells transiently transfected to express a particular class of PDE4 showed that the antisera and antibodies described here detected the appropriate PDE4 proteins in a class-specific fashion (results not shown).

Immunoprecipitation

Jurkat T-cell homogenates were resuspended in immunoprecipitation buffer (1 % Triton X-100/10 mM EDTA/100 mM NaH_2PO_4,$2H_2O$, 50 mM Hepes, pH 7.2) containing protease inhibitors (as added to the homogenization buffer; see above). This mixture was left on ice for 10 min and centrifuged at 13000 ***g*** for 4 min at 4 °C. After a similar preclearing step using Pansorbin, antiserum (1:50) was added to the supernatant and the sample was mixed for 2 h at 4 °C. A 100 μl volume of 10 % Pansorbin was added and mixed as above. After this, the sample was centrifuged on a Microfuge at 13000 ***g*** for 2 min, and the pellet was washed twice in immunoprecipitation buffer and then resuspended in PDE buffer for assay (see above).

RNA extraction

RNA was extracted from the cells using the Tri-reagent method. Preparation of first-strand cDNA was performed as described in the instruction manual supplied with the Pharmacia First strand kit, using a total reaction volume of 33 μl. Briefly, 5 μg of RNA, as determined by its absorbance at 260 nm, was denatured at 65 °C for 10 min and then incubated with murine reverse transcriptase, 6 mM dithiothreitol, 0.6 mM of each dNTP and 0.2 μg of the supplied poly(dT) primer [*Not*I-d$(T)_{18}$] for 60 min at 37 °C.

PCR protocol

Amplification was performed in 1 × PCR buffer (50 mM KCl, 20 mM Tris/HCl) with a total reaction volume of 50 μl. This contained final concentrations of 200 μM of each dNTP and 1.5 mM $MgCl_2$, together with 25 pmol of each primer, 5 units of *Taq* DNA polymerase and 3 μl of the cDNA. After the indicated cycles of denaturation and extension, a 5 μl aliquot from each reaction mixture was resolved by electrophoresis on a 1.8 % agarose gel and visualized by ethidium bromide staining under UV light. The primers used were as described below.

(i) Human PDE4A (hPDE4A), generic

The primers were: Sense-2067, ATGCAGACCTATCGCTCTGTCAGC; Antisense-2071, ACCATCGTGTCCACAGGGATGC. This employed 35 cycles at 95 °C for 1 min, 57 °C for 2 min and 72 °C for 3 min to detect a 506 bp fragment. These primers were designed to amplify a 3′ fragment found in all PDE4A species reported so far that encode an enzymically active protein (PDE-46, HSPDE4A4B, GenBank accession no. L20965; h6.1, HSPDE4A4C, GenBank U18087; HSPDE4A4A, GenBank M37744). The fragment amplified represents nucleotides 857–1362 in PDE-46 and nucleotides 407–912 in h6.1. It will also detect the non-active splice variant TM3 (GenBank L20967), amplifying nucleotides 743–1248.

(ii) hPDE-46, specific

Primers: Sense-2260, GTGGGGGCCGGATCCATGGAACCCCCGACC; Antisense-2261, GGTTCAACAGATATCTGAACTTGTGCGAGG. This employed 35 cycles at 95 °C for 1 min, 59 °C for 1 min and 72 °C for 90 s to detect a 817 bp fragment. These primers were designed to amplify a fragment unique to the largest reported PDE4A species to date, namely PDE-46 (HSPDE4A4B; GenBank accession no. L20965). The fragment amplified represents nucleotides 101–917 of PDE-46.

(iii) hPDE4B, generic

Primers: Sense-SE5, GACATTGCAACAGAAGACAAGTCCCC; Antisense-SE6, ACTCAAGTAACTGAAAGGCCAGGTGG. This employed 35 cycles at 95 °C for 1 min, 57 °C for 90 s and 72 °C for 2 min to detect a 168 bp fragment. These primers were designed to amplify a fragment characteristic of the two reported human PDE4B species, PDE-32 (GenBank accession no. L20971) and PDE-72 (GenBank L20966), comprising nucleotides 2422–2589 and 2311–2478 respectively.

(iv) hPDE4C

Primers: Sense-SE7, ATGGATGGTAAAGCCCTTTGGCTCTTGG; Antisense-SE8, GTCTCCCTAAATGGGTGGGAAAGTGAAG. This employed 35 cycles at 95 °C for 1 min, 58 °C for 2 min and 72 °C for 3 min to detect a 95 bp fragment. These primers were designed to amplify a fragment characteristic of the reported human PDE4C species (GenBank accession no. Z46632) which represents nucleotides 2279–2373.

(v) hPDE4D, generic

Primers: Sense-GR34, CCCTTGACTGTTATCATGCACACC; Antisense-GR35, GATCTACATCATGTATTGCACTGGC. This employed 40 cycles at 95 °C for 1 min, 55.3 °C for 2 min and 72 °C for 3 min to detect a 262 bp fragment. These primers were designed to amplify a 3′ fragment found in all human PDE4D species reported so far which encode an enzymically active protein; these are PDE4D1 (GenBank accession no. U50157; nucleotides 586–847) and PDE4D2 (GenBank U50158; nucleotides 500–761) reported by Nemoz et al. [36], and PDE43 (4D3; GenBank L20970; nucleotides 978–1239) and PDE39 (4D4; GenBank L20969; nucleotides 1674–1935) reported by Bolger et al. [23].

For all of the hPDE4 splice variants listed below, a common antisense primer was employed. This was Antisense-COM D-SE13 (GACTCCACTGATCTGAGACATTG). In all cases a common amplification protocol of 35 cycles at 95 °C for 1 min, 55 °C for 70 s and 72 °C for 100 s was employed.

(vi) hPDE4D1 splice variant

Sense PDE4D1-SE9, ATGGCCCCCTTTGAACTCGC. This allowed the detection of a 369 bp fragment which was found specifically in hPDE4D1 and represented nucleotides 64–432.

(vii) hPDE4D1/2 splice variants

Sense PDE4D1/2-SE16, AAGGAGCAGCCATCATGTGC. This allowed the detection of a 426 bp fragment found in hPDE4D1, representing nucleotides 7–432, and was also capable of detecting a 340 bp fragment in hPDE4D2 representing nucleotides 7–346.

(viii) hPDE4D3 splice variant

Sense PDE43-SE11, ATTGCCCACGATAGCTGCTC. This allowed the detection of a 800 bp fragment found specifically in PDE-43 representing nucleotides 25–824, as in the clone PDE43.

(ix) hPDE4D4 splice variant

Sense PDE39-SE10, AGCGCTACCTGTACTGTCG. This allowed the detection of a 764 bp fragment found specifically in PDE4D4 representing nucleotides 757–1520, as in the clone PDE39.

(x) Human β-actin

Sense-SE14, CATCGTCACCAACTGGGACGAC; Antisense-SE15, CGTGGCCATCTCTTGCTCGAAG. These were designed to amplify a 466 bp fragment representing nucleotides 263–728 of human β-actin (GenBank accession no. M10278). Such a fragment could be amplified under any of the above conditions but, as a routine, these were 35 cycles at 95 °C for 1 min, 55 °C for 70 s and 72 °C for 100 s.

(xi) PDE4B primers

PCR was carried out for PDE4B1 reflected by the clone PDE32 (GenBank accession no L20971; [23]) using the primers Sense-hB1 (AGCGGTGGTAGCGGTGACTC) and Antisense-hB2-601 (GCTGCGTGCAGGCTGTTGTG). These were aimed at amplifying a 680 bp product which reflects bases 805–1484 in the sequence of this splice variant. The reaction conditions used were 95 °C for 1 min, 59 °C for 2 min and 72 °C for 3 min for 35 cycles. Reverse transcription (RT)-PCR was also carried out for PDE4B2 reflected in the clone TM72 (GenBank accession no L20966; [23]) using the primers Sense-SE14 (ACCTTTCCTGGGCACAGCCAG) and Antisense-hB2-601. These were aimed at amplifying a 869 bp product which reflects bases 505–1373 in the sequence of this splice variant. The reaction conditions used were as described above.

RESULTS AND DISCUSSION

Pharmacological identification of PDE activity

In order to define which forms of PDE activity are present in human Jurkat T-cells, we employed a pharmacological approach using selective inhibitors and activators, as discussed in detail previously by us [37]. PDE1 activity was measured by performing PDE assays in the presence of EGTA, to chelate any endogenous Ca^{2+}, and then adding excess Ca^{2+}/calmodulin in order to determine the degree of stimulation of this isoform [9]. As shown in Table 1, low levels of PDE1 were present in these cells. At least three genes (*PDE*1A, 1B and 1C) encode PDE1 activity [38], and

Table 1 Pharmacological identification of PDE activity in Jurkat T-cells

Jurkat T-cell homogenates were assayed for PDE activity using 1 μM cAMP as substrate, and yielded basal activities of 18.2–19.8 pmol/min per mg of protein (range; $n = 5$ separate experiments using different cell homogenates and with PDE assays done in triplicate). IC_{50} values, maximal changes in activity and Hill coefficients (h) were determined from the dose–effect studies shown in Figure 1, with values given as means $\pm$ S.D. Changes in activity were determined at a single, maximally effective, concentration. n.d., not determined. As discussed previously by us [37], inhibition by rolipram indicates PDE4 activity and that by cilostimide indicates PDE3 activity. Stimulation by Ca^{2+}/calmodulin (50 μM and 20 ng/ml respectively) indicates the presence of PDE1 activity. Inhibition by EHNA indicates the presence of PDE2 activity. The latter was examined directly; in addition, an assessment was done of the action of EHNA on PDE activity in the presence of 10 μM cGMP, which will maximally activate any PDE2 activity present and so allow amplification of any action of EHNA. In the presence of 10 μM cGMP the PDE activity was 10.6–11.7 pmol/min per mg of protein (range; $n = 3$ separate experiments). IBMX was added at 500 μM. The number of separate determinations is indicated by n.

Ligand	IC_{50}	Activity change (%)	h	n
cGMP	0.9 $\pm$ 0.2 μM	-57 ± 5	0.7 $\pm$ 0.1	3
Cilostimide	178 $\pm$ 38 nM	-60 ± 4	1.0 $\pm$ 0.1	3
EHNA	n.d.	-5 ± 3	n.d.	3
EHNA + cGMP	3.2 $\pm$ 0.5 μM	-19 ± 5	1.1 $\pm$ 0.3	3
Rolipram	13 $\pm$ 7 nM	-25 ± 3	0.5 $\pm$ 0.1	3
Ca^{2+}/calmodulin	n.d.	$+18 \pm 5$	n.d.	5
IBMX	n.d.	-84 ± 6	n.d.	5

it would appear from RT-PCR transcript analyses that Jurkat T-cells express solely a PDE1B isoform [38a]. Low (1 μM) concentrations of cGMP stimulate the PDE activity of PDE2 and inhibit that of PDE3 [1,4,5,7]. Here we see that low concentrations of cGMP caused a profound, dose-dependent, inhibition of PDE activity (Figure 1a; Table 1), indicating that cGMP-inhibited PDE3 activity forms a major component of Jurkat cell PDE activity. The fact that the PDE3-selective inhibitor cilostimide [5] achieved a similar degree of inhibition (Figure 1b; Table 1) suggested that any cGMP-stimulated PDE2 activity must form a small component of the total PDE activity of these cells. This appears to be the case, as the PDE2-selective inhibitor EHNA [39–41] had little discernible inhibitory effect on homogenate PDE activity (Table 1). However, EHNA exerts its most profound inhibitory effect on the cGMP-stimulated state of PDE2 [41], and when monitoring this activity we were able to observe a small inhibitory effect of EHNA (Figure 1c; Table 1), indicating that PDE2 was expressed in Jurkat T-cells, albeit at low levels. The PDE4 selective inhibitor rolipram [2,3,8] caused a marked, dose-dependent, inhibition of Jurkat T-cell PDE activity (Figure 1d; Table 1).

It would appear (Table 1) that PDE4 and PDE3 together provided the major fraction of Jurkat T-cell PDE activity, accounting for $\sim 85\%$ of the total under the assay conditions used here. The residual activity is, presumably, contributed by the basal activities of PDE1 and PDE2, together with a possible small contribution by PDE7 [42], for which there is no selective inhibitor available.

Changes in PDE activity upon chronic elevation of intracellular cAMP levels

Elevation of Jurkat T-cell cAMP levels by chronic exposure to forskolin (Table 2) led to a profound increase in the homogenate PDE activity of these cells (Figure 2a). While no increases in the activities of either PDE1 or PDE2 (Figures 2b and 2c) were apparent, those of both PDE3 (Figures 2d and 2e) and PDE4 (Figure 2f) increased profoundly. A transient increase in PDE3 activity, which occurred over the first 45 min (Figure 2e), was followed by a sustained increase which began after approx. 3–4 h of exposure and continued through to 24 h (Figure 2d). The initial stimulatory effect on PDE3 activity may have been due to the cAMP-dependent phosphorylation of this enzyme, as such an action has been demonstrated by a number of investigators in various cell types [5,43–47]. The profound increase in PDE4 activity occurred after an initial lag period of 3–4 h, and levels remained elevated over the 24 h period studied here (Figure 2f).

The late-onset increases in both PDE3 and PDE4 activities, which began some 3–4 h after forskolin challenge, could be completely blocked by inhibiting transcription using actinomycin D (Table 2). This suggests that they were attributable to the induction of new protein. Actinomycin D treatment, however, did not block the rapid, transient, increase in PDE3 activity ($< 5\%$ change; $n = 3$; 40 min exposure to 100 μM forskolin in the presence compared with the absence of actinomycin D), consistent with this increase not involving enzyme induction. Furthermore, on using cholera toxin instead of forskolin to stimulate adenylate cyclase activity, we were similarly able to induce both PDE3 and PDE4 activities with a 9 h challenge (Table 2). This effect was also blocked by actinomycin D (Table 2). Incubation of cells with 8-bromo-cAMP also induced both PDE3 and PDE4 activities (Table 2), although to a lesser extent than seen with the other agents, which may reflect the metabolism of this compound. Such data are consistent with the elevation of cAMP levels in Jurkat T-cells leading to the increased expression of both PDE3 and PDE4 isoforms.

Challenge of Jurkat T-cells for 9 h with forskolin markedly elevated intracellular cAMP levels (Table 3; Figure 2g). Accumulation reached a maximum value after ~ 6 h and then began to decline before attaining a new steady-state level which was elevated above that seen in cells which had not been treated with forskolin (Figure 2g). The time at which the forskolin-elevated cAMP levels began to plateau and subsequently decline reflected the point at which intracellular PDE activity began to be elevated (Figure 2a). This elevation of intracellular cAMP concentrations was amplified ~ 5-fold if the non-selective PDE inhibitor IBMX was added together with forskolin (Table 3). Intriguingly, however, the PDE4-selective inhibitor rolipram was able to elicit a similar amplification to that seen with IBMX, whereas the PDE3-selective inhibitor cilostimide appeared to potentiate the forskolin-mediated increase in intracellular cAMP levels by only $\sim 50\%$ (Table 3). Such effects appear to be somewhat surprising in view of our observations that, in homogenate PDE assays, PDE3 activity was seen to be considerably greater than PDE4 activity. One possibility is that cilostimide did not achieve equilibrium concentrations inside the T-cells over the 9 h period. However, this seems somewhat unlikely, especially as cilostimide did cause an increase in cAMP levels and achieves inhibition of PDE3 at very low concentrations [7,8] (Table 1). Alternatively, in the intact cell these PDEs may be subject to regulatory constraints which alter their relative activities from those seen in homogenates. It is also possible that cAMP may be compartmentalized within these cells and that PDE4 activity regulates the bulk pool of cAMP. Indeed, this might explain the transient nature of the initial activation of PDE3 activity by forskolin (Figure 2e) if such an action was determined by a localized fraction of protein kinase A activity [48,49] controlled by a discrete pool of cAMP which was only transiently elevated above the threshold for protein kinase A activation. Whatever the explanation, our data imply that Jurkat T-cell PDE4 activity plays a prime role in controlling the bulk pool of cAMP produced by the forskolin-stimulated activation of adenylate cyclase.

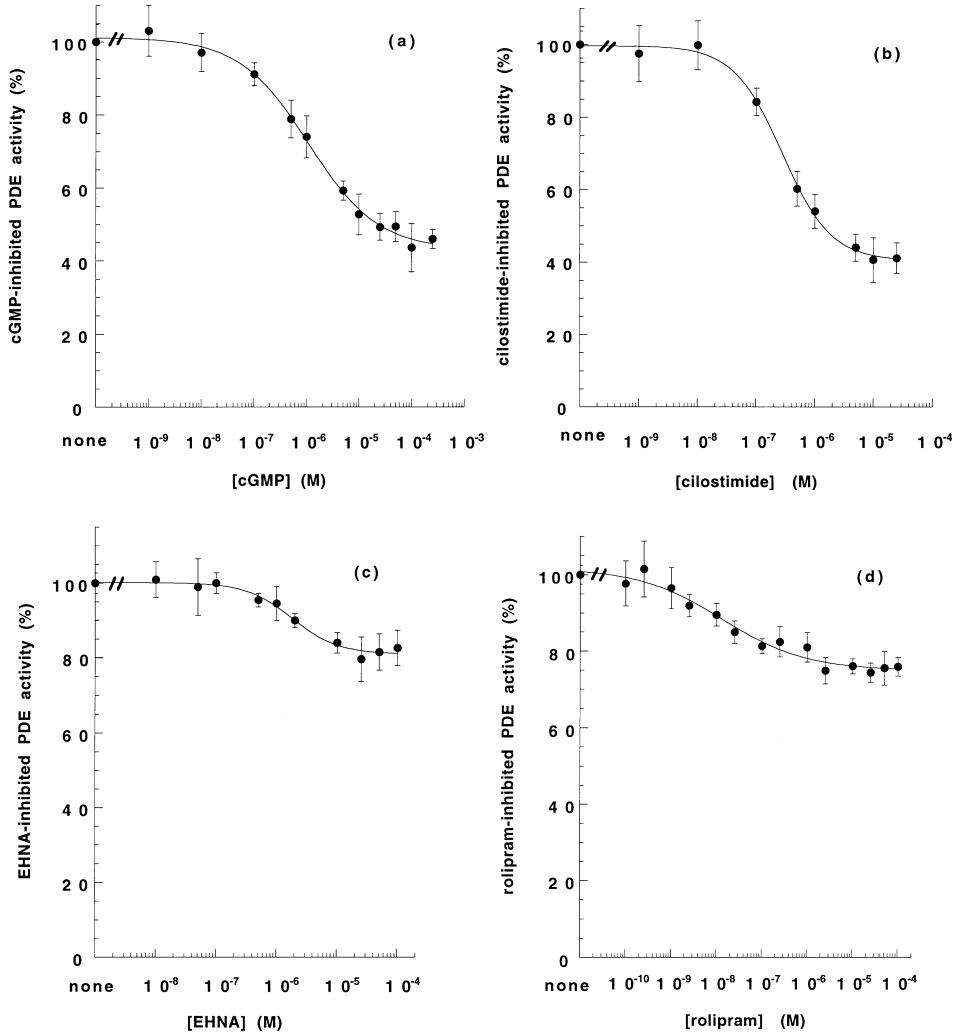

Figure 1 Action of selective ligands on Jurkat T-cell PDE activity

Homogenates of Jurkat T-cells were assayed for PDE activity using 1 μM cAMP as substrate. Basal homogenate PDE activity was 18.2–19.8 pmol/min per mg of protein (range; $n = 3$ separate experiments). Shown are percentage changes in activity from three experiments (means $\pm$ S.D.). (**a**) Dose-dependent changes in Jurkat T-cell PDE activity elicited by increasing concentrations of (unlabelled) cGMP. (**b**) Dose-dependent changes in Jurkat T-cell PDE activity elicited by increasing concentrations of the PDE3-selective inhibitor cilostimide. (**c**) Dose-dependent changes in Jurkat T-cell PDE activity elicited by increasing concentrations of the PDE2-selective inhibitor EHNA. Assays were carried out in the presence of 10 μM cGMP (unlabelled), which can be expected to maximally stimulate PDE2 activity and gave a control activity of 10.6–11.7 pmol/min per mg of protein (range; $n = 3$ separate experiments). (**d**) Dose-dependent changes in Jurkat T-cell PDE activity elicited by increasing concentrations of the PDE4-selective inhibitor rolipram. IC_{50} values and Hill coefficients for these data are given in Table 1.

Exposure of cells to the transcriptional inhibitor actinomycin D considerably enhanced, by $\sim$ 2.4-fold, the ability of forskolin to increase intracellular cAMP concentrations in Jurkat T-cells (Table 3). This implies that the forskolin-mediated induction of PDE activity was able to exert a considerable influence on intracellular cAMP levels. That addition of actinomycin D did not affect the forskolin-stimulated rise in cAMP assessed in the presence of rolipram (Table 3) showed that inhibition of transcription did not affect forskolin-stimulated adenylate cyclase activity.

Identification of the PDE4 isoforms affected by elevated cAMP levels

It is extremely unlikely that all of the possible PDE4 isoforms have been identified to date. This, coupled with observations that many PDE4 forms run anomalously on SDS/PAGE [27], makes it very difficult to attribute unambiguously immunoreactive species detected with antisera to particular PDE isoforms. In order to try to identify PDE4 isoforms occurring in Jurkat T-cells, we first used a PCR-based approach. For this we designed primers which we gauged would be generic for all active members of each of the four isoform families. This approach was taken in order to maximize the chances of detecting any unknown active PDE4 isoforms. The design of these 'generic', PDE4-class-specific primers was based on the fact that, within each PDE4 class, all active splice variants have identical sequences 3′ to the splice junction. Thus primer pairs were designed to detect a PDE4-subclass-specific portion of this 3′-coding region. Following this, we employed primers able to detect specific, known, splice variants. This strategy is shown schematically in Figure 3, and the primers used are given in the Materials and methods section. Finally, immunological methods were employed to identify protein products.

Table 2 Effect of actinomycin D on the increase in Jurkat T-cell PDE3 and PDE4 activities induced upon activation of adenylate cyclase by forskolin and cholera toxin

Jurkat T-cells were incubated with 100 μM forskolin (9 h), 1 μg/ml cholera toxin (6 h) or 100 μM 8-bromo-cAMP (9 h). In some experiments the transcriptional inhibitor actinomycin D (100 ng/ml) was added to incubations. After incubation, the cells were harvested and a homogenate prepared for assay of PDE activity using 1 μM cAMP as substrate. PDE3 activity was gauged as that fraction of the total PDE activity which was inhibited by 10 μM cilostimide. PDE4 activity was gauged as that fraction of the total PDE activity which was inhibited by 10 μM rolipram. Data are means $\pm$ S.D. for $n = 3$ separate experiments using different cell preparations. The change in PDE activity is given as a percentage of the activity seen in control cells (see Figure 1 for values). Thus 100% reflects a doubling of PDE activity. Significance of differences from control: * $P < 0.05$; ** $P < 0.001$.

	Change in activity (%)	
Treatment	PDE3	PDE4
Forskolin	131 $\pm$ 11**	215 $\pm$ 19**
Forskolin + actinomycin D	−38 $\pm$ 12*	11 $\pm$ 16
Actinomycin D	−12 $\pm$ 8	−18 $\pm$ 14
Cholera toxin	104 $\pm$ 14**	218 $\pm$ 49**
Cholera toxin + actinomycin D	18 $\pm$ 12	23 $\pm$ 15
8-Bromo-cAMP	69 $\pm$ 7**	58 $\pm$ 7**

Using sets of generic primers, we failed to identify transcripts for either PDE4B or PDE4C in RNA preparations from either control or forskolin-treated Jurkat T-cells (Figures 4b and 4c). The absence of the two known forms of human PDE4B (PDE-32 and PDE-72) [2,23,50] in both control and forskolin-treated Jurkat T-cells was also confirmed (results not shown) by using isoform-specific primers and by Western blotting procedures. These observations are in contrast with studies done on various monocyte cell lines [12,13] and in Sertoli cells [51], where elevation of cAMP levels induced PDE4B expression. Time-course studies done with Mono Mac 6 monocytes showed that the induction of PDE4B was transient, with maximal induction occurring $\sim$ 5 h after elevation of cAMP levels [13]. However, even when we studied cell extracts for transcripts and immunoreactive species at 1 h intervals over 9 h, we failed to observe any expression of PDE4B isoforms (results not shown).

We were able to demonstrate transcripts for both PDE4A and PDE4D (Figures 4a and 4d) in control Jurkat T-cells using sets of generic primers. However, probing RNA preparations from forskolin-treated cells for PDE4A transcripts (Figure 4a) consistently yielded signals of considerably lower intensity than those obtained using preparations from untreated cells (four separate experiments; signals obtained for β-actin transcripts showed no change). This suggests that levels of PDE4A were actually decreased upon elevation of intracellular cAMP. In order to examine this directly, we assessed the ability of a PDE4A-specific antiserum to immunoprecipitate PDE activity from solubilized Jurkat T-cells. In such experiments, PDE4 activity was indeed immunoprecipitated and, using optimal levels of antiserum, the maximum activity immunoprecipitated from control cells yielded a specific activity of 5.1 $\pm$ 0.2 pmol/min per mg of protein ($n = 3$ experiments; units expressed relative to T-cell homogenate PDE activity). This fraction of activity was remarkably similar to the total rolipram-inhibited PDE component determined using Jurkat T-cell homogenates (4.9 $\pm$ 0.5 pmol/min per mg of protein; $n = 3$) suggesting that, in control cells, PDE4A activity provides the major, if not the sole, PDE4 activity. However, in cells treated with forskolin for 9 h, the immunoprecipitated PDE4A activity recorded was some 3.1 $\pm$ 0.3 pmol/min per mg of protein (mean $\pm$ S.D.; $n = 3$ separate experiments using different cell preparations; units expressed relative to T-cell homogenate PDE activity), implying a decrease in PDE4A expression of $\sim$ 40 %. In each instance > 96 % of the immunoabsorbed activity was inhibited upon addition of 10 μM rolipram, indicating that this was indeed exclusively PDE4 activity. Such a reduction in the amount of presumed PDE4A activity seen in forskolin-treated cells was consistent with the decreased signal seen by RT-PCR transcript analysis (Figure 4a). In analyses done by immunoblotting for PDE4A forms, we identified a single (118 $\pm$ 4 kDa) immunoreactive species whose intensity was considerably diminished (45 $\pm$ 6 %; $n = 3$ experiments) in extracts from forskolin-treated cells (Figure 5a). This immunoreactive species, however, migrated considerably faster on SDS/PAGE than did PDE-46 (HSPDE4A4B), an established, active, product of the human *PDE*4A gene [23] which migrated as an $\sim$ 125 kDa species (Figure 5a). We think it unlikely that such a difference was due to proteolysis, as a single species of reproducible size was obtained in all our PDE4A immunoblot studies done with Jurkat T-cells. This was apparent when cells were boiled directly in SDS/PAGE sample buffer or if this was done subsequent to extraction in the presence of protease inhibitors (results not shown). Consistent with the notion that this may reflect a novel splice variant, when we used PCR primers designed to detect the extreme 5′ region of PDE-46 (HSPDE4A4B), we failed to obtain a signal in extracts from Jurkat T-cells (Figure 6a). A further indication that this may be a novel splice variant is that the IC_{50} value for inhibition of this species by rolipram is $\sim$ 50-fold lower than that seen for h6.1 (HSPDE4A4C) [25,26] and PDE-46 (HSPDE4A4B) [35], indicating a particularly potent action of this selective inhibitor on the T-cell PDE4A isoform. Certainly, the rat *PDE*4*A* gene yields at least three distinct, active, splice variants [52] and, while to date only PDE-46 (HSPDE4A4B) has been shown to provide an active product from this locus in human beings, two inactive splice variants have been identified [23,53], suggesting that alternative splicing is an inherent attribute of the *PDE*4*A* gene.

Analysis of PDE4D transcripts by RT-PCR using a set of generic primers detected a weak signal in RNA preparations from untreated Jurkat cells (Figure 4d). However, using forskolin-treated cells we consistently obtained a very much stronger signal (Figure 4d). This implied an increase in the level of PDE4D transcripts upon elevation of intracellular cAMP concentrations. Alternative splicing of the rat *PDE*4*D* gene has been well documented by Conti and co-workers [3], and this has also been noted for the *PDE*4*D* gene from humans [2,3]. At least four different, active, splice variants have been identified to date (see [23,36]). Using sets of primers able to detect each of these reported variants, we failed to detect any signals for PDE4D3 and PDE4D4 species in either untreated or forskolin-treated cells (results not shown). However, we were able to obtain a signal for PDE4D1 in RNA extracts from control cells, although this was rather weak (Figures 6b and 6c). The effect of forskolin treatment was to increase dramatically the signal for PDE4D1 (Figures 6b and 6c) and also to allow the detection of novel transcripts for PDE4D2 (Figure 6c). Immunoblot analysis using PDE4D-specific antisera failed to identify any signal for PDE4D species in extracts from untreated Jurkat cells (Figure 5b). This suggests that the expression of PDE4D species in untreated cells is minimal, consistent with our contention that the predominant component of PDE4 activity under such conditions is due to a PDE4A isoform. However, in forskolin-treated cells we obtained a strong signal for a species of 67 $\pm$ 2 kDa (Figure 5b) which co-migrated with PDE4D1 expressed in transfected COS cells. This is consistent with our RT-PCR analyses, which implied cAMP-

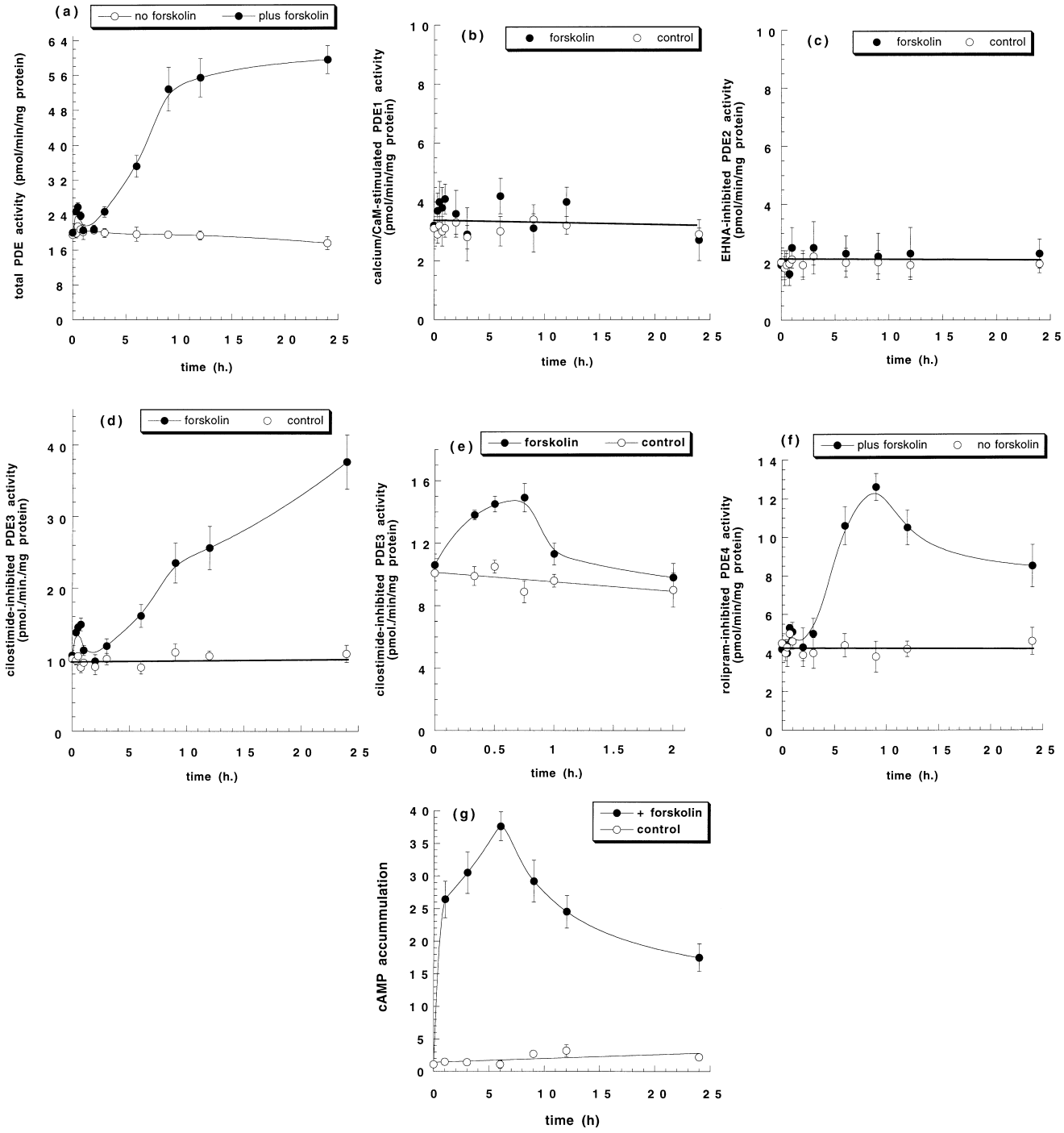

Figure 2 Forskolin-induced changes in Jurkat T-cell PDE activity

Jurkat T-cells were incubated for the indicated times in either the absence or the presence of 100 μM forskolin. After this time, cells were washed, harvested and homogenized as described in the Materials and methods section. The PDE activity of homogenates was assessed using 1 μM cAMP as substrate. Selective activators and inhibitors were employed to measure the activity of the different PDE classes, as discussed in detail previously by us [37]. Total Jurkat T-cell homogenate PDE activity is shown in (**a**). Changes in PDE1 activity (**b**) were assessed by determining the incremental increase in PDE activity achieved on addition of Ca^{2+}/calmodulin (CaM) (50 μM and 20 ng/ml respectively) to assays, i.e. the Ca^{2+}/calmodulin-stimulated component only was measured. Changes in PDE2 activity (**c**) were determined by measuring the incremental inhibition of PDE activity achieved by the selective inhibitor EHNA for assays carried out in the presence of a maximally stimulating concentration of cGMP (10 μM) [41]. PDE3 activity (**d**) was determined by assessing the fractional inhibition achieved using the selective inhibitor cilostimide (10 μM), with the first 2 h shown in detail in (**e**). PDE4 activity (**f**) was determined by assessing the fractional inhibition of PDE activity achieved using the selective inhibitor rolipram (10 μM). Jurkat T-cell intracellular cAMP levels (**g**) are shown as pmol of cAMP/10^6 cells. Data are given for control (○) and forskolin-treated (●) cells in all panels, and are means ± S.D. for triplicate assays done in a single experiment. These data are typical of experiments done three times.

Table 3 Forskolin-stimulated increases in Jurkat T-cell intracellular cAMP levels

Jurkat T-cells were cultured for 9 h in the presence of no added ligand (control) or the indicated combinations of 100 μM forskolin, 10 μM rolipram, 10 μM cilostimide, 1 mM IBMX and 100 ng/ml actinomycin D (Act-D). After this time the cells were harvested and their intracellular cAMP levels were determined. Data are means $\pm$ S.D. for $n = 3$ separate experiments using different cell preparations. 'Fold change' indicates the fold potentiation of the forskolin-induced elevation of intracellular cAMP levels.

Ligands	[cAMP] (pmol of cAMP/10^6 cells)	Fold change
None (control)	1.6 ± 0.4	–
Forskolin	29.2 ± 2.6	(1)
Forskolin + rolipram	154 ± 8	5.3
Forskolin + Act-D	70.0 ± 5.3	2.4
Forskolin + Act-D + rolipram	158 ± 9	5.4
Forskolin + cilostimide	44.2 ± 3.8	1.5
Forskolin + IBMX	148 ± 12	5.1

mediated induction of the PDE4D1 splice variant. Immunoblot studies, however, also identified a weakly expressed species, with an apparent size of 65 ± 2 kDa, which consistently migrated just below that identified as PDE4D1 (Figure 5b). This species seems most likely to be PDE4D2, as it is highly related to PDE4D1 but has a small internal deletion of 86 bp in its 5′ alternatively spliced region which would make the encoded protein product slightly smaller than PDE4D1. Furthermore, we were able to identify transcripts for PDE4D2 in extracts from forskolin-treated cells (Figure 6c). We also routinely detected a weakly staining species at 75 ± 3 kDa in PDE4D immunoblot studies done on forskolin-treated Jurkat cells (Figure 5b). Whether this reflects an as yet unreported PDE4D splice variant remains to be seen.

Conclusions

Chronic elevation of cAMP levels in Jurkat T-cells caused a profound, time-dependent, increase in overall cellular PDE activity. This effect was predominantly achieved through regulation of the expression of PDE3 and PDE4 isoforms, although a transient activation of PDE3 was also noted. The effects of chronic elevation of cAMP levels on PDE4 expression were exclusively targeted to actions on genes encoding PDE4A and PDE4D. Intriguingly, despite a profound increase in PDE4 activity, we observed a marked decrease in the expression of the single PDE4A isoform which appeared to supply the majority, if not all, of the PDE4 activity in control Jurkat T-cells. This decrease in the expression of PDE4A in Jurkat T-cells contrasts with the effect of chronically elevated cAMP levels on monocyte cell lines [12,13], where increased expression of a PDE4A species was seen. However, in those cell lines the PDE4A splice variant expressed appeared to reflect PDE-46 (HSPDE4A4B) [13]. Such data may thus signal differences in the control of expression of splice variants in various cell types in response to elevation of intracellular cAMP concentrations. This decrease in the expression of the PDE4A isoform was more than compensated for, however, by the profound induction of the PDE4D1 isoform, together with a much smaller level of induction of the PDE4D2 isoform. This induction of PDE4D isoforms is somewhat reminiscent of that noted in Sertoli cells [10], where elevation of cAMP levels caused a profound induction of both PDE4D1 and PDE4D2 isoforms. Increased PDE4D1 levels were also noted in Mono Mac 6 monocytes in response to chronic elevation of cAMP concentrations [13]. However, in marked contrast with these observations, high resting levels of PDE4D expression were

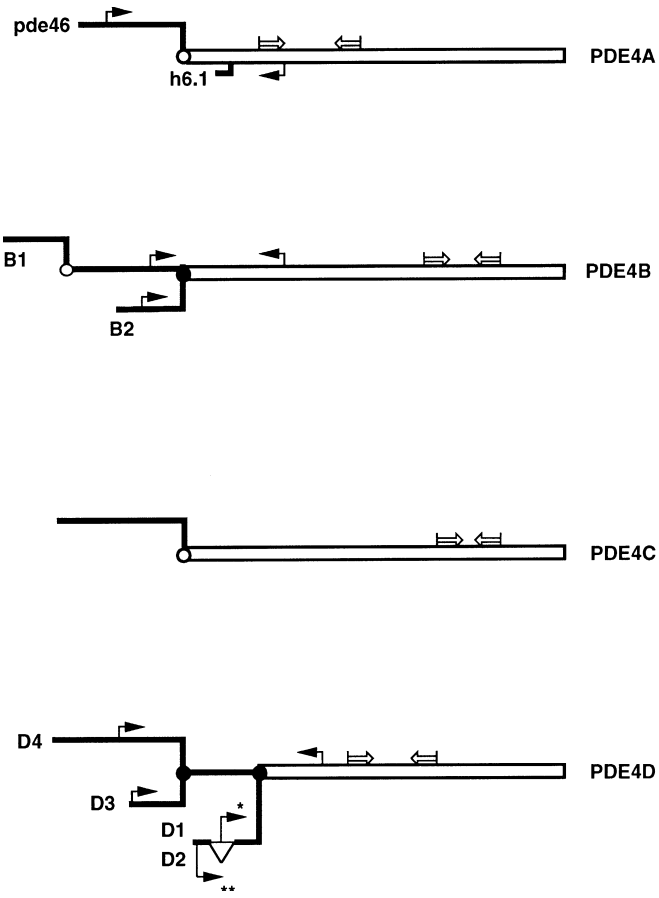

Figure 3 Schematic representation of primers used to analyse human PDE4 transcripts by RT-PCR

The primers used in this study for RT-PCR analyses of human PDE4 transcripts are shown schematically. The PDE4 products of the four genes are shown with presumptive (○) (on the basis of analogy with either rat or other PDE4 families) and established (■) splice junctions indicated, and the names of the established active splice variants are given [2,3]. Open arrows indicate the relative positions of the generic primer pairs used to identify the presence of transcripts encoding active members of a PDE4 subclass. Filled arrows indicate the relative positions of primer pairs used to identify the presence of specific splice variants. These are given for the sense (left to right) and antisense (right to left) directions. The PDE4A schematic shows the two identified active species. These are PDE-46 (HSPDE4A4B; GenBank accession no. L20965) [23], which is analogous to the rat PDE4 isoform RPDE6 (RNPDE4A5; GenBank L27057) found expressed in brain [27], and the truncated species h6.1 (HSPDE4A4C, GenBank U18087), which is closely related to HSPDE4A4A (GenBank M37744). The fragment amplified using the generic primers represents nucleotides 857–1362 in PDE-46 and 407–912 in h6.1. The fragment amplified with the PDE-46-specific primers represents nucleotides 101–917. The PDE4B schematic shows the two splice variants PDE4B1 (GenBank L20971) and PDE4B2 (GenBank L20966) [23]. Specific primers amplified a product which reflected bases 805–1484 in PDE4B1 and bases 505–1373 in PDE4B2. Generic primers amplified an identical sequence found in transcripts of both products which reflected nucleotides 2422–2589 and 2311–2478 in PDE4B1 and PDE4B2 respectively. The PDE4C schematic shows the single reported form identified [24] to date (GenBank Z46632), but indicates a common point at which, by analogy with other PDE4 species, a splice junction might be expected. The generic primers used were designed to amplify a fragment which represents nucleotides 2279–2373. The PDE4D schematic shows the human splice variants identified to date [3,23,36], which show analogy with the rat forms [3]. Generic primers were designed to amplify a 3′ fragment found in all human PDE4D species reported so far which encode an enzymically active protein: PDE4D1 (GenBank U50157; nucleotides 586–847), PDE4D2 (GenBank U50158; nucleotides 500–761), PDE4D3 (GenBank L20970; nucleotides 978–1239) and PDE4D4 (GenBank L20969; nucleotides 1674–1935). Specific primers amplified fragments for PDE4D1 (nucleotides 64–432), PDE4D1 + PDE4D2 (nucleotides 7–432 and nucleotides 7–346 respectively), PDE4D3 (nucleotides 25–82) and PDE4D4 (nucleotides 757–1520). The single asterisk indicates the position of the sense primer used to detect PDE4D1 specifically. This is placed with the 86 bp sequence which is deleted from PDE4D2 [36]. The double asterisk indicates the position of the sense primer used to detect PDE4D1 and PDE4D2.

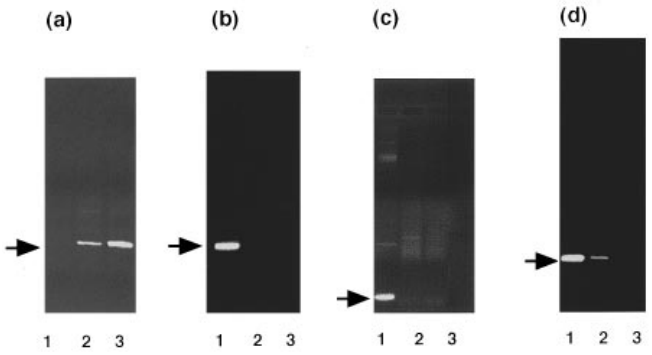

Figure 4 RT-PCR analysis of Jurkat T-cells using generic primers

RNA was prepared from Jurkat T-cells that either had or had not been treated for 9 h with 100 μM forskolin. The samples were then analysed in a RT-PCR procedure using sets of generic primers for the four PDE4 classes, as described in the Materials and methods section and shown schematically in Figure 3. In (**a**), PDE4A generic primers were used which allowed the detection of a fragment of the predicted size (506 bp) in control cells (track 3) and in forskolin-treated cells (track 2), but not in RNA-free/blank experiments. In (**b**), PDE4B generic primers were used which allowed the detection of a fragment of the predicted size (168 bp) in RNA extracts from COS cells transfected with the human PDE4B species PDE-32 [23] (track 1), but no signal was obtained using RNA from either forskolin-treated cells (track 2) or untreated Jurkat T-cells (track 3). In (**c**), PDE4C generic primers were used which allowed the detection of a fragment of the predicted size (95 bp) using RNA extracts from *Saccharomyces cerevisiae* transfected so as to express a human PDE4C species [24] (track 1), but no signal was obtained using RNA from either forskolin-treated cells (track 2) or untreated Jurkat T-cells (track 3). In (**d**), PDE4D generic primers were used which allowed the detection of a fragment of the predicted size (262 bp) using RNA extracts from forskolin-treated Jurkat T-cells (track 1), but with a much reduced signal using RNA from untreated Jurkat T-cells (track 2) and no signal from experiments with no added RNA (track 3). These data are typical of experiments done at least three times using different cell incubations. RNA extracts from treated and untreated Jurkat T-cells were matched in each instance, and gave identical signals for amplification of a fragment of β-actin (see the Materials and methods section; results not shown).

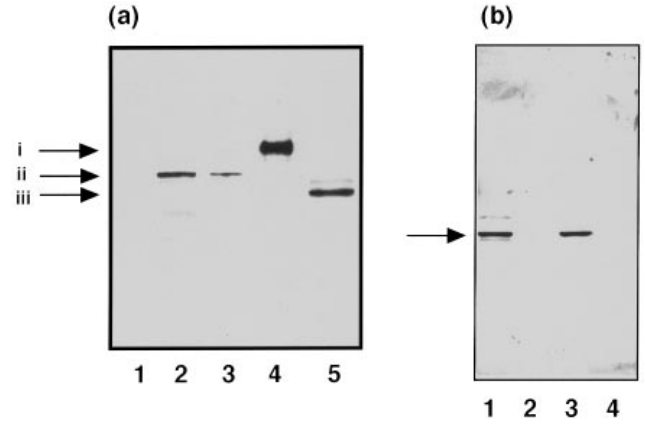

Figure 5 Immunoblotting of Jurkat T-cells for PDE4A and PDE4D

Immunoblots for PDE4A and PDE4D immunoreactive species are shown. In (**a**), antiserum specific for PDE4A was used to probe extracts of untreated Jurkat T-cells (track 2), forskolin-treated Jurkat T-cells (track 3), COS cells transfected to express human PDE-46 [23] (track 4), COS cells transfected to express human h6.1 [25,26] (track 5) and no addition (track 1). The arrows labelled i, ii and iii indicate PDE-46, Jurkat cell PDE4A and h6.1 respectively. In (**b**), antiserum specific for PDE4D was used to probe extracts of forskolin-treated Jurkat T-cells (track 1), untreated Jurkat T-cells (track 2), COS cells transfected to express human PDE4D1 [23] (track 3) and no addition (track 4). The arrow indicates PDE4D.

seen in U973 monocytes, and these were not affected by elevation of intracellular cAMP levels [12]. Such observations give additional support to the notion [3] that cAMP-responsive elements

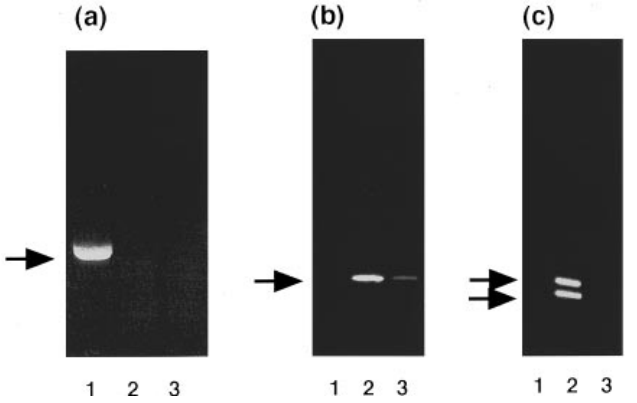

Figure 6 RT-PCR analysis of Jurkat T-cells using splice variant specific primers

(**a**) Experiments using primers specific for the established human PDE4A splice variant PDE-46 (HSPDE4A4B; GenBank accession no. L20965), which identified transcripts from COS cells transfected to express PDE-46 (track 1) but not from either forskolin-treated (track 2) or untreated (track 3) Jurkat T-cells. (**b**) Experiments using primers specific for the human PDE4D1 splice variant, which identified a very strong signal for a transcript of the predicted size of 369 bp in forskolin-treated Jurkat T-cells (track 2), but only an extremely weak signal in untreated cells (track 3) and no signal in experiments with no added RNA (track 1). (**c**) Experiments using primers able to detect both the human PDE4D1 and PDE4D2 splice variants. These identified a strong signal for PDE4D1and PDE4D2 transcripts of the predicted sizes of 426 bp and 340 bp respectively in forskolin-treated cells (track 2), with no signal evident either in untreated cells or in RNA-free experiments. These results are typical of experiments done at least three times using different cell incubations. RNA extracts from treated and untreated Jurkat T-cells were matched in each instance, and gave identical signals for amplification of a fragment of β-actin (see the Materials and methods section; results not shown).

determine the expression of specific PDE4D splice variants, as well as demonstrating that inhibitory effects can be exerted on *PDE*4A gene expression.

The functional significance of changes in the expression of specific PDE4 splice variants remains to be ascertained. However, the observations that PDE4 isoforms appear to exhibit marked differences in their activity [27,34,52], intracellular targeting [27,34,52], protein–protein interactions [54] and regulation by covalent modification [3] might mean that there are specific functional consequences for the form of these changes. This might explain why the pattern of changes in PDE4 isoform expression in response to elevated intracellular cAMP levels appears to have cell-specific attributes. Thus, such induction of PDE isoforms is likely to reflect a cell-specific adaptive mechanism. This may have implications for the use of therapeutic regimens which lead to elevated intracellular cAMP levels, and also for disease states which involve adenylate cyclase activation.

This work was supported by a grant from the MRC (U.K.). S.E. was supported by Mustafa Kemal University. We thank Dr. K. M. Ferguson (ICOS Corp., Bothell, WA, U.S.A.) for generously donating monoclonal antibodies, which were developed by Cathy Farrell and Sharon Wolda.

REFERENCES

1 Beavo, J. A. (1995) Physiol. Rev. **75**, 725–748
2 Bolger, G. (1994) Cell. Signalling **6**, 851–859
3 Conti, M., Nemoz, G., Sette, C. and Vicini, E. (1995) Endocr. Rev. **16**, 370–389
4 Thompson, W. J. (1991) Pharmacol. Ther. **51**, 13–33
5 Manganiello, V. C., Taira, M., Degerman, E. and Belfrage, P. (1995) Cell. Signalling **7**, 445–455
6 Ashton, M. J., Cook, D. C., Fenton, G., Karlsson, J. A., Palfreyman, M. N., Raeburn, D., Ratcliffe, A. J., Souness, J. E., Thurairatnam, S. and Vicker, N. (1994) J. Med. Chem. **37**, 1696–1703

7 Nicholson, C. D. and Shahid, M. (1994) Pulm. Pharmacol. **7**, 1–17
8 Torphy, T. J., Barnette, M. S., Hay, D. W. P. and Underwood, D. C. (1994) Environ. Health Perspect. **102**, 79–84
9 Manganiello, V. C., Murata, T., Taira, M., Belfrage, P. and Degerman, E. (1995) Arch. Biochem. Biophys. **322**, 1–13
10 Sette, C., Vicini, E. and Conti, M. (1994) J. Biol. Chem. **269**, 18271–18274
11 Swinnen, J. V., Joseph, D. R. and Conti, M. (1989) Proc. Natl. Acad. Sci. U.S.A. **86**, 8197–8201
12 Torphy, T. J., Zhou, H. L., Foley, J. J., Sarau, H. M., Manning, C. D. and Barnette, M. S. (1995) J. Biol. Chem. **270**, 23598–23604
13 Verghese, M. W., McConnell, R. T., Lenhard, J. M., Hamacher, L. and Jin, S.-L. C. (1995) Mol. Pharmacol. **47**, 1164–1171
14 Bach, M.-A., Fournier, C. and Bach, J.-F. (1975) Ann. N.Y. Acad. Sci **249**, 316–327
15 Kammer, G. M. (1988) Immunol. Today **9**, 222–229
16 Kaye, J. and Ellenberger, D. L. (1992) Cell **71**, 423–435
17 Chen, D. and Rothenberg, E. V. (1994) J. Exp. Med. **179**, 931–942
18 Anastassiou, E. D., Paliogianni, F., Balow, J. P., Yamada, H. and Boupas, D. T. (1992) J. Immunol. **148**, 2845–2852
19 Cook, S. J. and McCormick, F. (1993) Science **262**, 1069–1072
20 Wu, H. and Parsons, J. (1993) J. Cell Biol. **120**, 1417–1426
21 Hafner, S., Adler, H. S. and Mischak, H. (1994) Mol. Cell. Biol. **14**, 6696–6703
22 Hsueh, Y.-P. and Lai, M.-Z. (1995) J. Biol. Chem. **270**, 18094–18098
23 Bolger, G., Michaeli, T., Martins, T., St John, T., Steiner, B., Rodgers, L., Riggs, M., Wigler, M. and Ferguson, K. (1993) Mol. Cell. Biol. **13**, 6558–6571
24 Engels, P., Sullivan, M., Muller, T. and Lubbert, H. (1995) FEBS Lett. **358**, 305–310
25 Sullivan, M., Egerton, M., Shakur, Y., Marquardson, A. and Houslay, M. D. (1994) Cell. Signalling **6**, 793–812
26 Wilson, M., Sullivan, M., Brown, N. and Houslay, M. D. (1994) Biochem. J. **304**, 407–415
27 McPhee, I., Pooley, L., Lobban, M., Bolger, G. and Houslay, M. D. (1995) Biochem. J. **310**, 965–974
28 Bradford, M. M. (1976) Anal. Biochem. **72**, 248–254
29 Marchmont, R. J. and Houslay, M. D. (1980) Biochem. J. **187**, 381–392
30 Rutten, W. J., Schoot, B. M. and Dupont, J. S. H. (1973) Biochim. Biophys. Acta **315**, 378–383
31 Thompson, W. J. and Appleman, M. M. (1971) Biochemistry **10**, 311–316
32 Whetton, A. D., Needham, L., Dodd, N. J. F., Heyworth, C. M. and Houslay, M. D. (1983) Biochem. Pharmacol. **32**, 1601–1608
33 Laemmli, U.K. (1970) Nature (London) **227**, 680–685
34 Shakur, Y., Wilson, M., Pooley, L., Lobban, M., Griffiths, S. L., Campbell, A. M., Beattie, J., Daly, C. and Houslay, M. D. (1995) Biochem. J. **306**, 801–809
35 Huston, E., Pooley, L., Julien, P., Scotland, G., McPhee, I., Sullivan, M., Bolger, G. and Houslay, M. D. (1996) J. Biol. Chem., in the press
36 Nemoz, G., Zhang, B., Sette, C. and Conti, M. (1996) FEBS Lett. **384**, 97–102
37 Spence, S., Rena, G., Sweeney, G. and Houslay, M. D. (1995) Biochem. J. **310**, 975–982
38 Loughney, K., Martins, T. J., Harris, E. A. S., Sadhu, K., Hicks, J. B., Sonnenburg, W. K., Beavo, J. A. and Ferguson, K. (1996) J. Biol. Chem. **271**, 796–806
38a Spence, S., Rena, G., Sullivan, M., Erdogan, S. and Houslay, M. D. (1997) Biochem. J. **321**, 157–163
39 Podzuweit, T., Nennstiel, P. and Muller, A. (1995) Cell. Signalling **7**, 733–738
40 Mery, P. F., Pavoine, C., Pecker, F. and Fischmeister, R. (1995) Mol. Pharmacol. **48**, 121–130
41 Michie, A. M., Lobban, M., Muller, T., Harnett, M. M. and Houslay, M. D. (1996) Cell. Signalling **8**, 97–110
42 Michaeli, T., Bloom, T. J., Martins, T., Loughney, K., Ferguson, K., Riggs, M., Rodgers, L., Beavo, J. A. and Wigler, M. (1993) J. Biol. Chem. **268**, 12925–12932
43 Anderson, N. G., Kilgour, E. and Houslay, M. D. (1989) Biochem. J. **262**, 867–872
44 Kilgour, E., Anderson, N. G. and Houslay, M. D. (1989) Biochem. J. **260**, 27–36
45 Gettys, T. W., Vine, A. J., Simonds, M. F. and Corbin, J. D. (1988) J. Biol. Chem. **263**, 10359–10363
46 Macphee, C. H., Reifsnyder, D. H., Moore, T. A., Lerea, K. M. and Beavo, J. A. (1988) J. Biol. Chem. **263**, 10353–10358
47 Smith, C. J., Vasta, V., Degerman, E., Belfrage, P. and Manganiello, V. C. (1991) J. Biol. Chem. **266**, 13385–13390
48 Scott, J. D. and McCartney, S. (1994) Mol. Endocrinol. **8**, 5–11
49 Rubin, C. S. (1994) Biochim. Biophys. Acta **1224**, 467–479
50 McLaughlin, M. M., Cieslinski, L. B., Burman, M., Torphy, T. J. and Livi, G. P. (1993) J. Biol. Chem. **268**, 6470–6476
51 Swinnen, J. V., Tsikalas, K. E. and Conti, M. (1991) J. Biol. Chem. **266**, 18370–18377
52 Bolger, G., McPhee, I. and Houslay, M. D. (1996) J. Biol. Chem. **271**, 1065–1071
53 Horton, Y. M., Sullivan, M. and Houslay, M. D. (1995) Biochem. J. **308**, 683–691
54 O'Connell, J. C., McCallum, J. F., McPhee, I., Wakefield, J., Houslay, E. S., Wishart, W., Bolger, G., Frame, M. and Houslay, M. D. (1996) Biochem. J. **318**, 255–262

Received 27 June 1996/15 August 1996; accepted 23 August 1996